

Unnormalized Optimal Transport

Stanley Osher

UCLA, 2019

Goals

- ▶ A simple and natural way to compare densities with unnormalized/unbalanced total mass.



W. Gangbo



W. Li



S. Osher



M. Puthawala

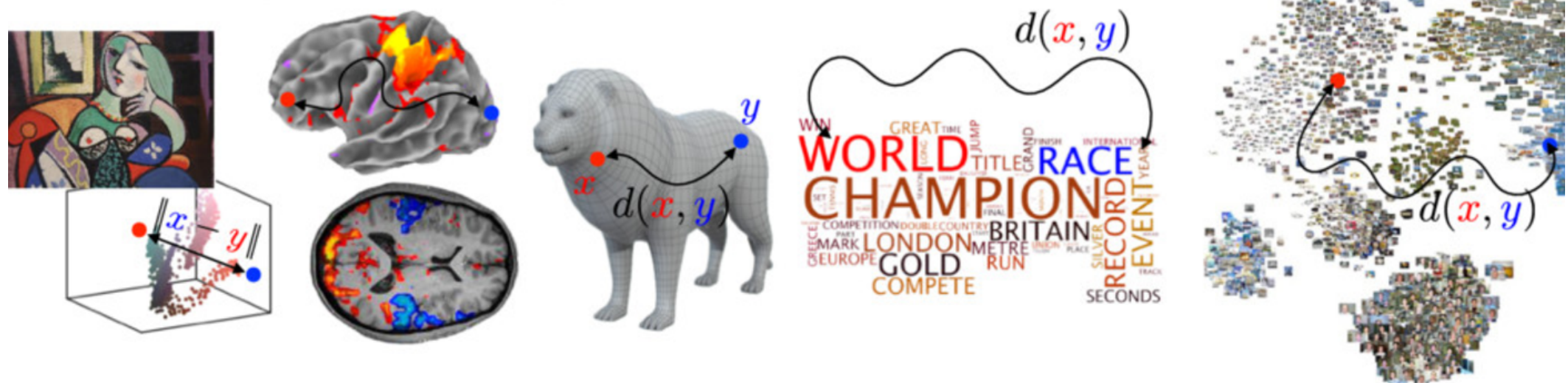
GLOP

Distance among histograms

Measuring the closeness among density functions (histograms) plays crucial roles in applications, such as

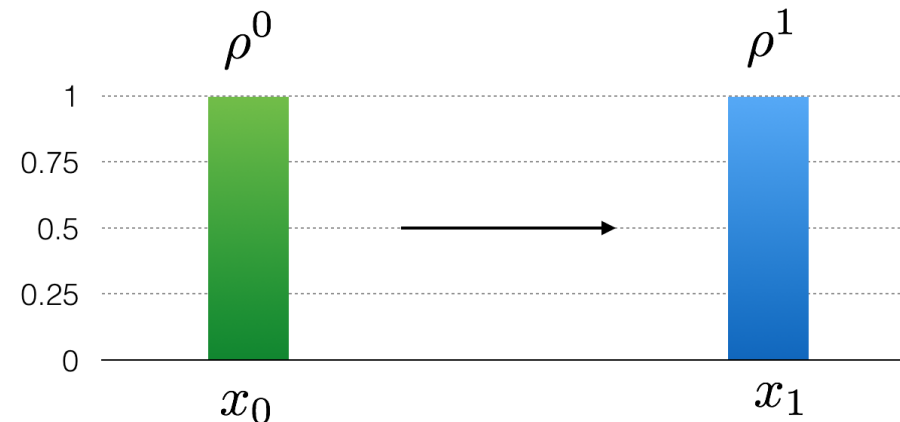
- ▶ Image processing and Inverse problems (Li et. al 2018, Yang et.al 2018, Puthawala et.al. 2018);
- ▶ Machine learning (Lin et. al 2018);
- ▶ Mean field games (Chow et. al 2018).

- *Probability distributions and histograms*
→ images, vision, graphics and machine learning, ...



Transport Distance

Optimal transport provides a particular distance (W) among histograms, which relies on the distance on sample spaces (ground cost c).



Denote $X_0 \sim \rho^0 = \delta_{x_0}$, $X_1 \sim \rho^1 = \delta_{x_1}$. Compare

$$W(\rho^0, \rho^1) = \inf_{\pi \in \Pi(\rho^0, \rho^1)} \int \int c(x, y) \pi(x, y) dx dy = c(x_0, x_1);$$

Vs

$$\text{TV}(\rho^0, \rho^1) = \int_{\Omega} |\rho^0(x) - \rho^1(x)| dx = 2;$$

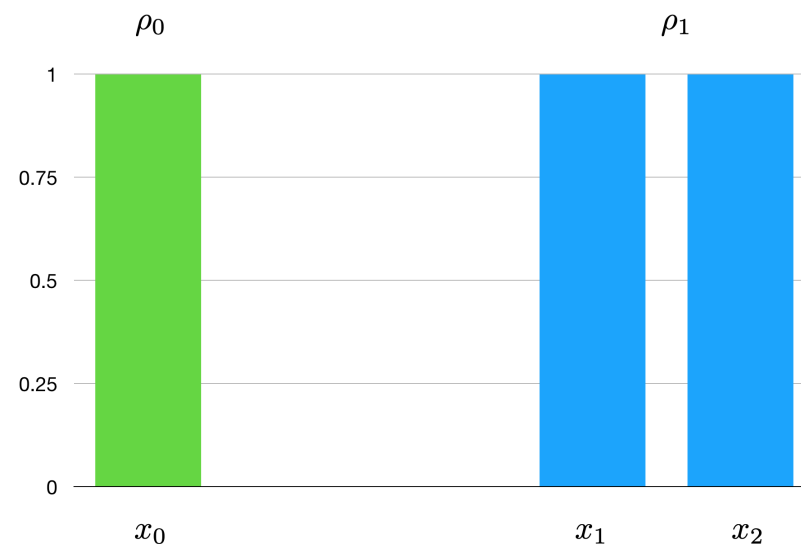
Vs

$$\text{KL}(\rho^0 \| \rho^1) = \int_{\Omega} \rho^0(x) \log \frac{\rho^0(x)}{\rho^1(x)} dx = \infty.$$

Goals: Unnormalized Transport

Main Questions

In real applications such as inverse problems and image processing, one needs to measure unnormalized/unbalanced densities.



Solutions:

We propose a **simple and natural** modification of optimal transport to compare unnormalized/unbalanced densities, and introduce an efficient numerical scheme.

Related studies

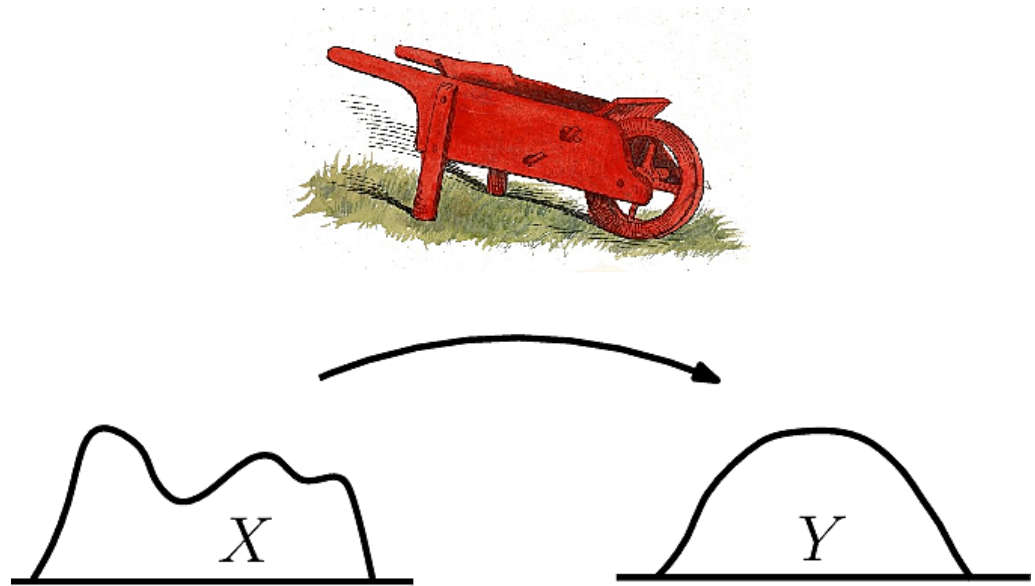
- ▶ Wasserstein-Fisher-Rao metric, L. Chizat, G. Peyre, B. Schmitzer, and F.-X. Vialard, *Journal of Functional analysis*.
- ▶ Hellinger-Kantorovich metric, M. Liero, A. Mielke, and G. Savare, *Inventiones mathematicae*.
- ▶ Free boundaries in optimal transport and Monge-Ampere obstacle problems, L. Caffarelli and R. McCann, *Annals of Mathematics*.
- ▶ Transport and equilibrium in non-conservative systems, L. Chayes and H. K. Lei, *Advances in Differential Equations* .
- ▶ Transport based image morphing with intensity modulation, J. Maas, M. Rumpf and S. Simon, *SSVM*.

Compared to the above approaches, unnormalized OT has a closed-form

Unnormalized Monge-Ampere equation,

is able to be solved by a very simple and efficient *Primal-Dual algorithm* (Chambolle-Pock).

Optimal transport



What is the optimal way to move or transport the mountain with shape X , density $\rho^0(x)$ to another shape Y with density $\rho^1(y)$?

The optimal transport problem was first introduced by Monge in 1781, relaxed by Kantorovich by 1940. It introduces a particular metric on probability set. In literatures, the problem is often named Earth Mover's distance, Monge-Kantorovich problem and Wasserstein metric, etc.

Normalized Optimal Transport

Balanced case

$$\int_{x \in A} \rho_1(x) dx = \int_{T(x) \in A} \rho_0(x) dx,$$

where T is a smooth one to one map on \mathbb{R}^d :

$$\det(\nabla T(x)) \rho_1(T(x)) = \rho_0(x),$$

This is called the Jacobian equation underdetermined.

L^p Monge–Kantorovich–Wasserstein distance

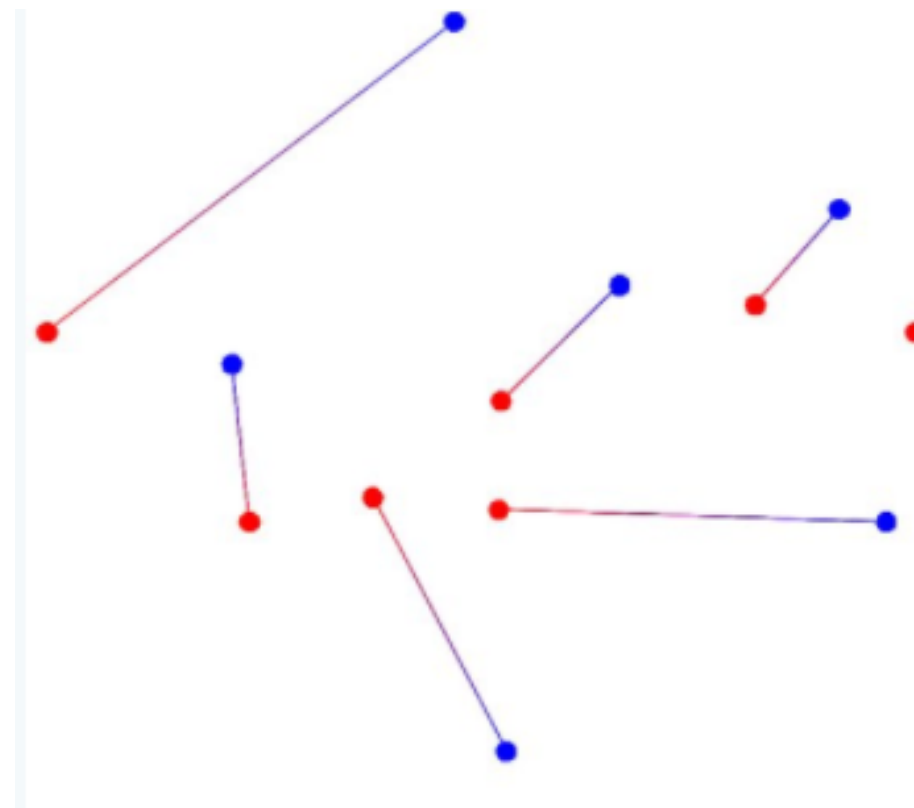
Given two measures ρ^0, ρ^1 with equal mass. Consider

$$(W_p(\rho_0, \rho_1))^p = \inf_T \int_{\Omega} \|x - T(x)\|^p \rho_0(x) dx$$

where the infimum is among all transport maps T , which transfers $\rho^0(x)$ to $\rho^1(x)$, i.e.

$$\rho_0(x) = \rho_1(T(x)) \det(\nabla T(x)) .$$

The minimizer T is the optimal transfer, which solves L^p Monge-Kantorovich problem.



Monge–Ampere equation

Brenier showed for $p = 2$, uniqueness of optimal transfer T , such that

$$T(x) = \nabla \Psi(x).$$

This means

$$\det(\text{Hess}\Psi(x))\rho_1(\nabla \Psi(x)) = \rho_0(x).$$

It is the Monge-Ampere equation, which is hard to solve directly.

Dynamical formulation



Benamou–Brenier

The distance has an important fluid dynamics formulation (Benamou-Brenier 2000). Then the square of L^2 Kantorovich distance satisfies

$$(W_2(\rho_0, \rho_1))^2 = \inf_{\rho, v} \int_0^1 \int \|v(t, x)\|^2 \rho(t, x) dx dt ,$$

where infimum runs over the continuity equation, such that

$$\partial_t \rho_t + \nabla \cdot (\rho v) = 0 , \quad \rho_0 = \rho_0 , \quad \rho_1 = \rho_1 .$$

Here the minimizer satisfies

$$v(t, x) = \nabla \Phi(t, x),$$

and

$$\frac{\partial}{\partial t} \Phi(t, x) + \frac{1}{2} \|\nabla \Phi(t, x)\|^2 = 0.$$

We shall focus on this formulation, and further propose an extension.

Unnormalized Optimal Transport

Define

$$UW_p(\mu_0, \mu_1)^p = \inf_{v, \mu, f} \int_0^1 \int_{\Omega} \|v(t, x)\|^p \mu(t, x) dx dt + \frac{1}{\alpha} \int_0^1 |f(t)|^p dt \cdot |\Omega|$$

such that the dynamical constraint: the unnormalized continuity equation holds

$$\partial_t \mu(t, x) + \nabla \cdot (\mu(t, x) v(t, x)) = f(t),$$

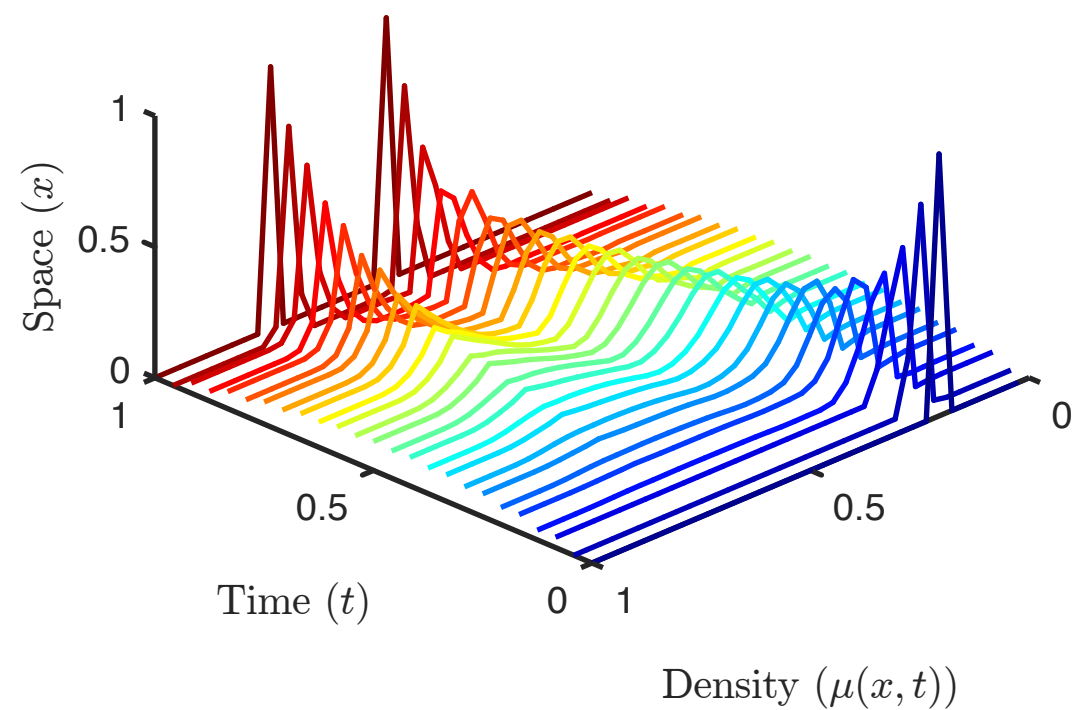
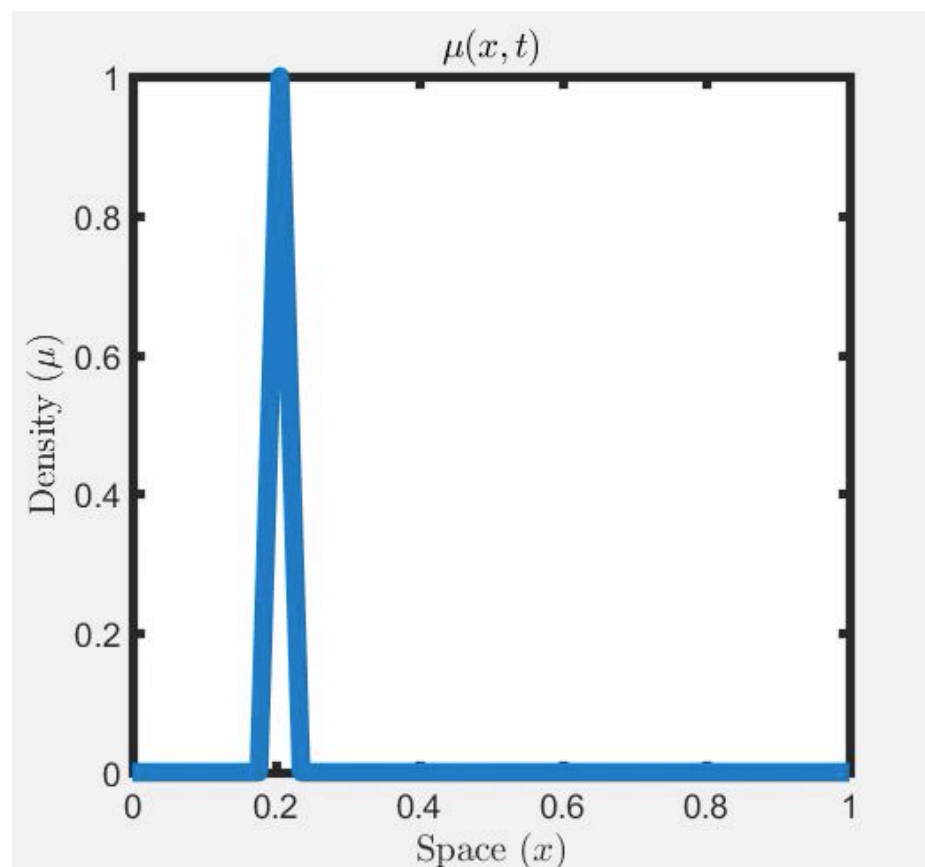
with

$$\mu(0, x) = \mu_0(x), \quad \mu(1, x) = \mu_1(x).$$

In this talk, we mainly consider $p = 1, 2$.

Snowing and melting

The source function $f(t)$ introduce the precisely co-dimensional one variation into the density space.



New metric

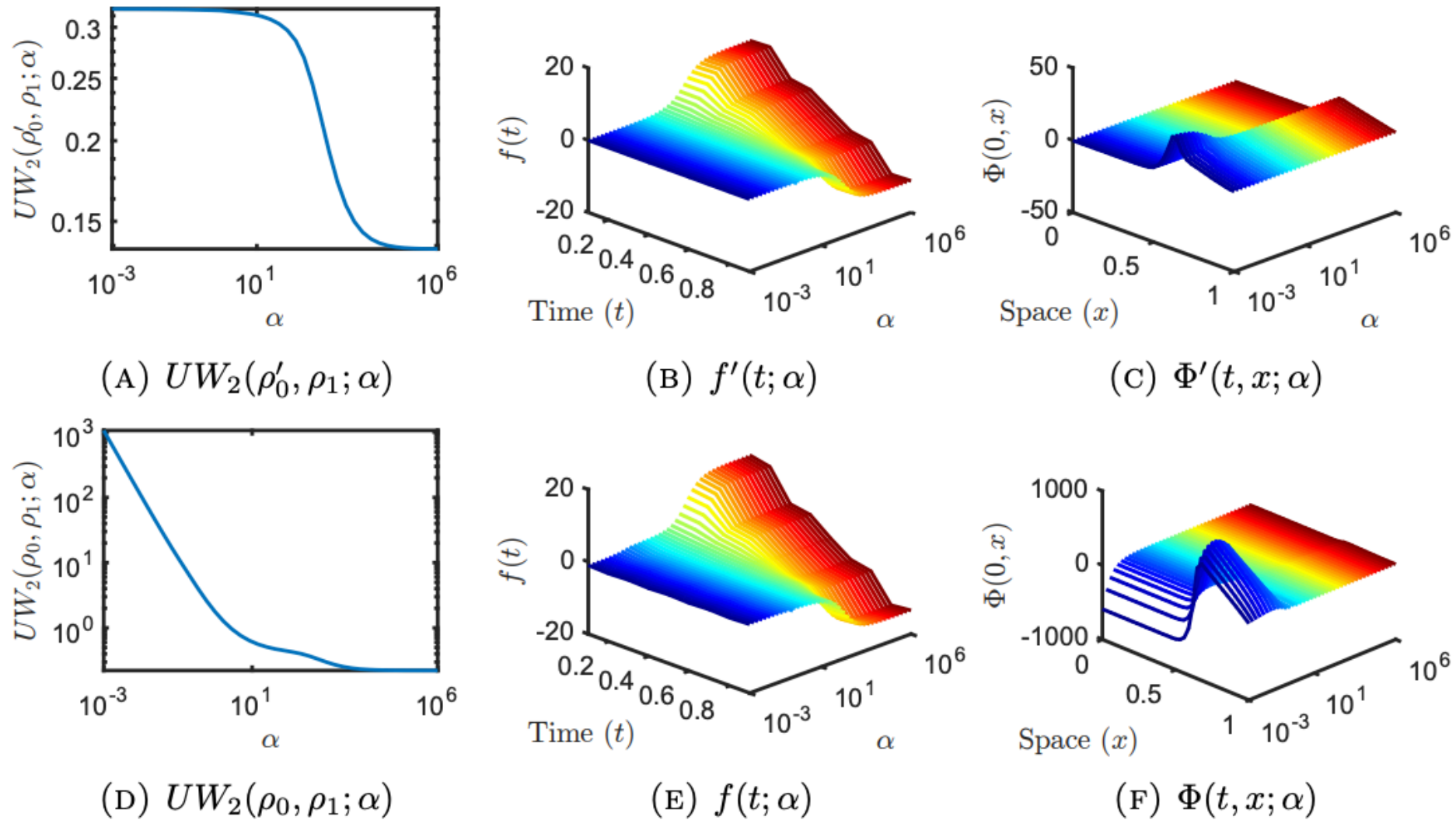


FIGURE 2. A plot of the asymptotic behavior of UW_2 in α with balanced and unbalanced inputs. Balanced: (A) $UW_2(\rho'_0, \rho_1; \alpha)$, (B) $f'(t; \alpha)$, (C) $\Phi'(t, x; \alpha)$, and unbalanced: (D) $UW_2(\rho_0, \rho_1; \alpha)$, (E) $f(t; \alpha)$, (F) $\Phi(t, x; \alpha)$.

Unnormalized L^1 Wasserstein metric

Let $p = 1$:

$$\text{UW}_1(\mu_0, \mu_1) = \inf_{v, f(t)} \left\{ \int_0^1 \int_{\Omega} \|v\| \mu dx dt + \frac{1}{\alpha} \int_0^1 |f(t)| dt \cdot |\Omega| : \right. \\ \left. \partial_t \mu + \nabla \cdot (\mu v) = f(t) \right\}.$$

Time independent solution

Denote

$$m(x) = \int_0^1 v(t, x) \mu(t, x) dt,$$

with the fact

$$\int_0^1 f(t) dt = c = \frac{1}{|\Omega|} \left(\int_{\Omega} \mu_1(x) dx - \int_{\Omega} \mu_0(x) dx \right).$$

then by Jensen's inequality and integrating the time variable t , we obtain

$$\begin{aligned} & \text{UW}_1(\mu_0, \mu_1) \\ &= \inf_m \left\{ \int_{\Omega} \|m(x)\| dx + \frac{1}{\alpha} \left| \int_{\Omega} \mu_0(x) dx - \int_{\Omega} \mu_1(x) dx \right| : \right. \\ & \quad \left. \mu_1(x) - \mu_0(x) + \nabla \cdot m(x) = \frac{1}{|\Omega|} \left(\int_{\Omega} \mu_1(x) dx - \int_{\Omega} \mu_0(x) dx \right) \right\}. \end{aligned}$$

Closed form solution

In one space dimension on the interval $\Omega = [0, 1]$, the L^1 unnormalized Wasserstein metric has the following explicit solution:

$$\begin{aligned} \text{UW}_1(\mu_0, \mu_1) = & \int_{\Omega} \left| \int_0^x \mu_1(y) dy - \int_0^x \mu_0(y) dy - x \int_{\Omega} (\mu_1(z) - \mu_0(z)) dz \right| dx \\ & + \frac{1}{\alpha} \left(\left| \int_{\Omega} \mu_1(z) dz - \int_{\Omega} \mu_0(z) dz \right| \right). \end{aligned}$$

Algorithm

In high dimensional sample space, the L_1 unnormalized OT problem forms

$$\underset{m}{\text{minimize}} \quad \|m\|_{1,2} \quad \text{subject to} \quad \text{div}(m) + \mu^1 - \mu^0 = c.$$

It is a particular example of **compressed sensing**. It can be solved easily by Primal-Dual algorithm (Chambolle and Pock).

Primal-Dual updates

Consider the Lagrangian of UOT:

$$\mathcal{L}(m, \Phi) = \int_0^1 \int_{\Omega} \|m\| + \Phi(\operatorname{div}(m) + \mu^1 - \mu^0) dx,$$

where $\Phi(t, x)$ is the Lagrange multiplier of the unnormalized continuity equation. The primal-dual update forms

$$\begin{cases} m^{k+1}(t, x) = \arg \inf_m \mathcal{L} + \frac{1}{2\tau_1} \int_0^1 \int_{\Omega} \|m(t, x) - m^k(t, x)\|^2 dx dt \\ \tilde{\Phi}^{k+1}(t, x) = \arg \sup_{\Phi} \mathcal{L} - \frac{1}{2\tau_2} \int_0^1 \int_{\Omega} \|\Phi(t, x) - \Phi^k(t, x)\|^2 dx dt \end{cases}$$

where m, Φ are taking the gradient descent, ascent directions respectively, with τ_1, τ_2 being the stepsizes.

Algorithm: 2 line codes

Primal-dual method

1. For $k = 1, 2, \dots$ Iterates until convergence
 2. $m^{k+1} = \text{shrink}(m^k + \mu \nabla \Phi^k, \mu)$;
 3. $\Phi^{k+1} = \Phi^k + \tau \{ \text{div}(2m^{k+1} - m^k) + p^1 - p^0 + c \}$;
 4. End
-

Here the shrink operator for the ground metric

$$\text{shrink}(y, \alpha) := \frac{y}{\|y\|} \max\{\|y\| - \alpha, 0\} , \quad \text{where } y \in \mathbb{R}^d .$$

Examples

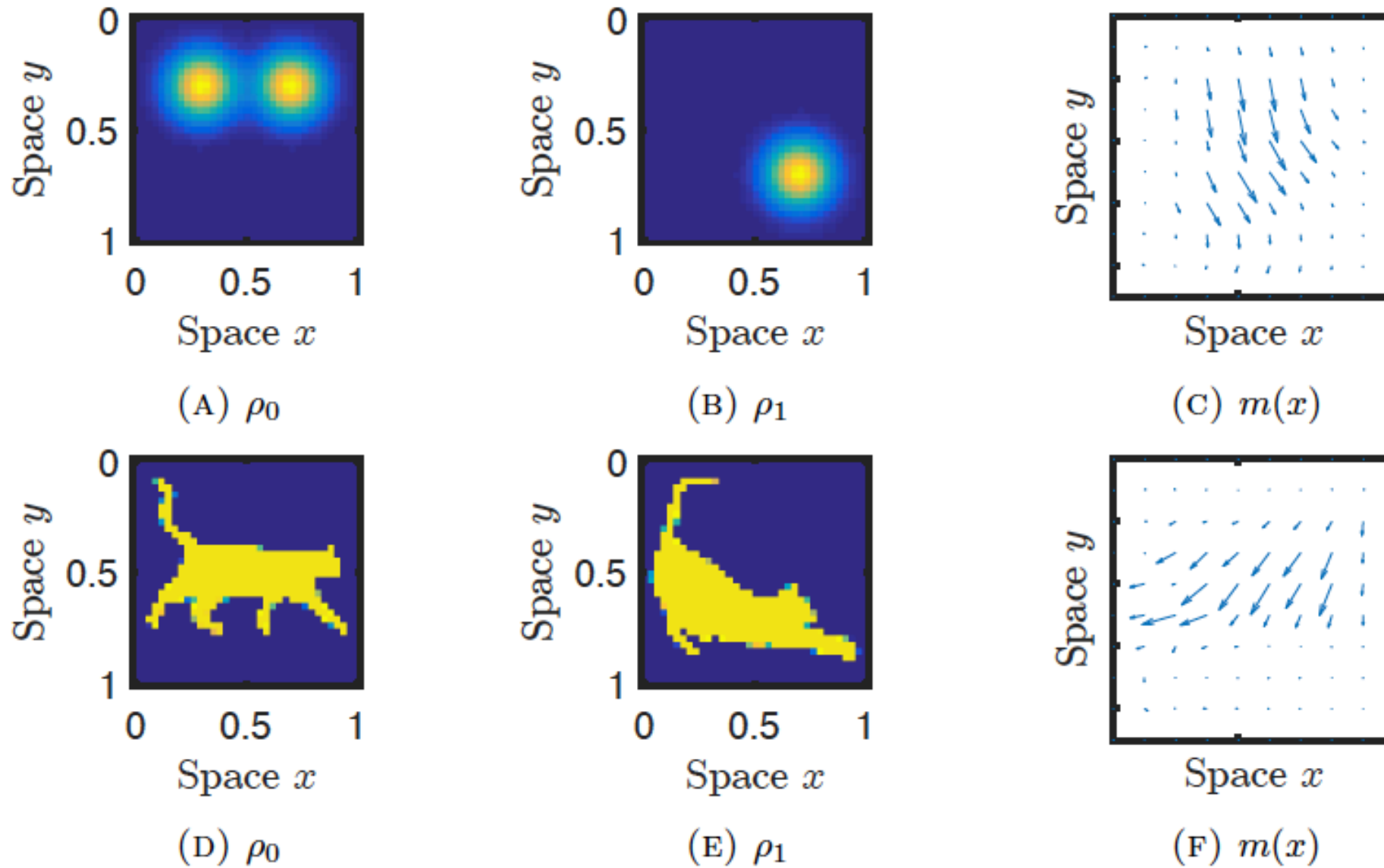


FIGURE 5. Plots of the ρ_0 , ρ_1 and $m(x)$ for $UW_1(\rho_0, \rho_1)$ for the two gaussian movement (A) ρ_0 , (B) ρ_1 , (C) $m(x)$ and two (D) ρ_0 , (E) ρ_1 , (F) $m(x)$.

Unnormalized L^2 Wasserstein metric

Let $p = 2$:

$$\text{UW}_2(\mu_0, \mu_1) = \inf_{v, f(t)} \left\{ \int_0^1 \int_{\Omega} \|v\|^2 \mu dx dt + \frac{1}{\alpha} \int_0^1 f(t)^2 dt \cdot |\Omega| : \right. \\ \left. \partial_t \mu + \nabla \cdot (\mu v) = f(t) \right\}.$$

Minimizer system

The minimizer $(v(t, x), \mu(t, x), f(t))$ for UOT problem satisfies

$$v(t, x) = \nabla \Phi(t, x), \quad f(t) = \alpha \frac{1}{|\Omega|} \int_{\Omega} \Phi(t, x) dx,$$

and

$$\begin{cases} \partial_t \mu(t, x) + \nabla \cdot (\mu(t, x) \nabla \Phi(t, x)) = \alpha \frac{1}{|\Omega|} \int_{\Omega} \Phi(t, x) dx \\ \partial_t \Phi(t, x) + \frac{1}{2} \|\nabla \Phi(t, x)\|^2 = 0 \\ \mu(0, x) = \mu_0(x), \quad \mu(1, x) = \mu_1(x). \end{cases}$$

Unnormalized Monge-Ampere equation

Denote

$$\Psi(x) = \frac{1}{2}\|x\|^2 + \Phi(0, x),$$

Following the Hopf-Lax formula, the minimizer of unnormalized OT satisfies

$$\begin{aligned} & \mu(1, \nabla \Psi(x)) \text{Det}(\nabla^2 \Psi(x)) - \mu(0, x) \\ &= \alpha \int_0^1 \text{Det}\left(t \nabla^2 \Psi(x) + (1-t)\mathbb{I}\right) \cdot \\ & \quad \int_{\Omega} \left(\Psi(y) - \frac{\|y\|^2}{2} + \frac{t\|\nabla \Psi(y) - y\|^2}{2} \right) \text{Det}\left(t \nabla^2 \Psi(y) + (1-t)\mathbb{I}\right) dy dt. \end{aligned}$$

Unnormalized Kantorovich problem

$$\frac{1}{2} \text{UW}_2(\mu_0, \mu_1)^2 = \sup_{\Phi} \left\{ \int_{\Omega} \Phi(1, x) \mu(1, x) dx - \int_{\Omega} \Phi(0, x) \mu(0, x) dx \right. \\ \left. - \frac{\alpha}{2} \int_0^1 \left(\int_{\Omega} \Phi(t, x) dx \right)^2 dt \right\}$$

where the supremum is taken among all $\Phi: [0, 1] \rightarrow \Omega$ satisfying

$$\partial_t \Phi(t, x) + \frac{1}{2} \|\nabla \Phi(t, x)\|^2 \leq 0.$$

Algorithm

Denote $m(t, x) = \mu(t, x)v(t, x)$. Consider the Lagrangian of UOT:

$$\begin{aligned}\mathcal{L}(m, \mu, f, \Phi) = & \int_0^1 \int_{\Omega} \frac{\|m(t, x)\|^2}{2\mu(t, x)} dt dx + \frac{1}{2\alpha} \int_0^1 f(t)^2 dt \\ & + \int_0^1 \int_{\Omega} \Phi(t, x) \left(\partial_t \mu(t, x) + \nabla \cdot m(t, x) - f(t) \right) dx dt,\end{aligned}$$

where $\Phi(t, x)$ is the Lagrange multiplier of the unnormalized continuity equation. This formulation allows us to apply the primal dual algorithm for

$$\inf_{m, \mu} \sup_{f, \Phi} \mathcal{L}(m, \mu, f, \Phi).$$

Primal-Dual updates

$$\left\{ \begin{array}{l} m^{k+1}(t, x) = \arg \inf_m \mathcal{L} + \frac{1}{2\tau_1} \int_0^1 \int_{\Omega} \|m(t, x) - m^k(t, x)\|^2 dx dt \\ \mu^{k+1}(t, x) = \arg \inf_{\mu} \mathcal{L} + \frac{1}{2\tau_1} \int_0^1 \int_{\Omega} \|\mu(t, x) - \mu^k(t, x)\|^2 dx dt \\ f^{k+1}(t) = \arg \inf_f \mathcal{L} + \frac{1}{2\tau_1} \int_0^1 \|f(t) - f^k(t)\|^2 dt \\ \tilde{\Phi}^{k+1}(t, x) = \arg \sup_{\Phi} \mathcal{L} - \frac{1}{2\tau_2} \int_0^1 \int_{\Omega} \|\Phi(t, x) - \Phi^k(t, x)\|^2 dx dt \\ (\tilde{m}, \tilde{\mu}, \tilde{f}) = 2(m^{k+1}, \mu^{k+1}, f^{k+1}) - (m^k, \mu^k, f^k) \end{array} \right.$$

Algorithm

Algorithm: Primal-Dual method for Unnormalized OT

1. **For** $k = 1, 2, \dots$ Iterate until convergence
 2. $m^{k+1}(t, x) = \frac{\mu^k(t, x)}{\mu^k(t, x) + \tau_1} \left(\tau_1 \nabla \Phi(t, x) + m^k(t, x) \right);$
 3. $\mu^{k+1}(t, x) = \arg \inf_{\mu} \left(\frac{\|m^k\|^2}{2\mu} - \partial_t \Phi \cdot \mu + \frac{1}{2\tau_1} |\mu - \mu^k|^2 \right) (t, x);$
 4. $f^{k+1}(t) = \frac{\alpha}{\alpha + \tau_1} \left(\tau_1 \int_{\Omega} \Phi(t, x) dx + f^k(t) \right);$
 5. $\Phi^{k+1}(t, x) = \Phi^k(t, x) + \tau_2 \left(\partial_t \tilde{\mu}^{k+1}(t, x) + \nabla \cdot \tilde{m}(t, x) - \tilde{f}(t) \right);$
 6. $(\tilde{m}, \tilde{\mu}, \tilde{f}) = 2(m^{k+1}, \mu^{k+1}, f^{k+1}) - (m^k, \mu^k, f^k);$
 7. **end**
-

Example I

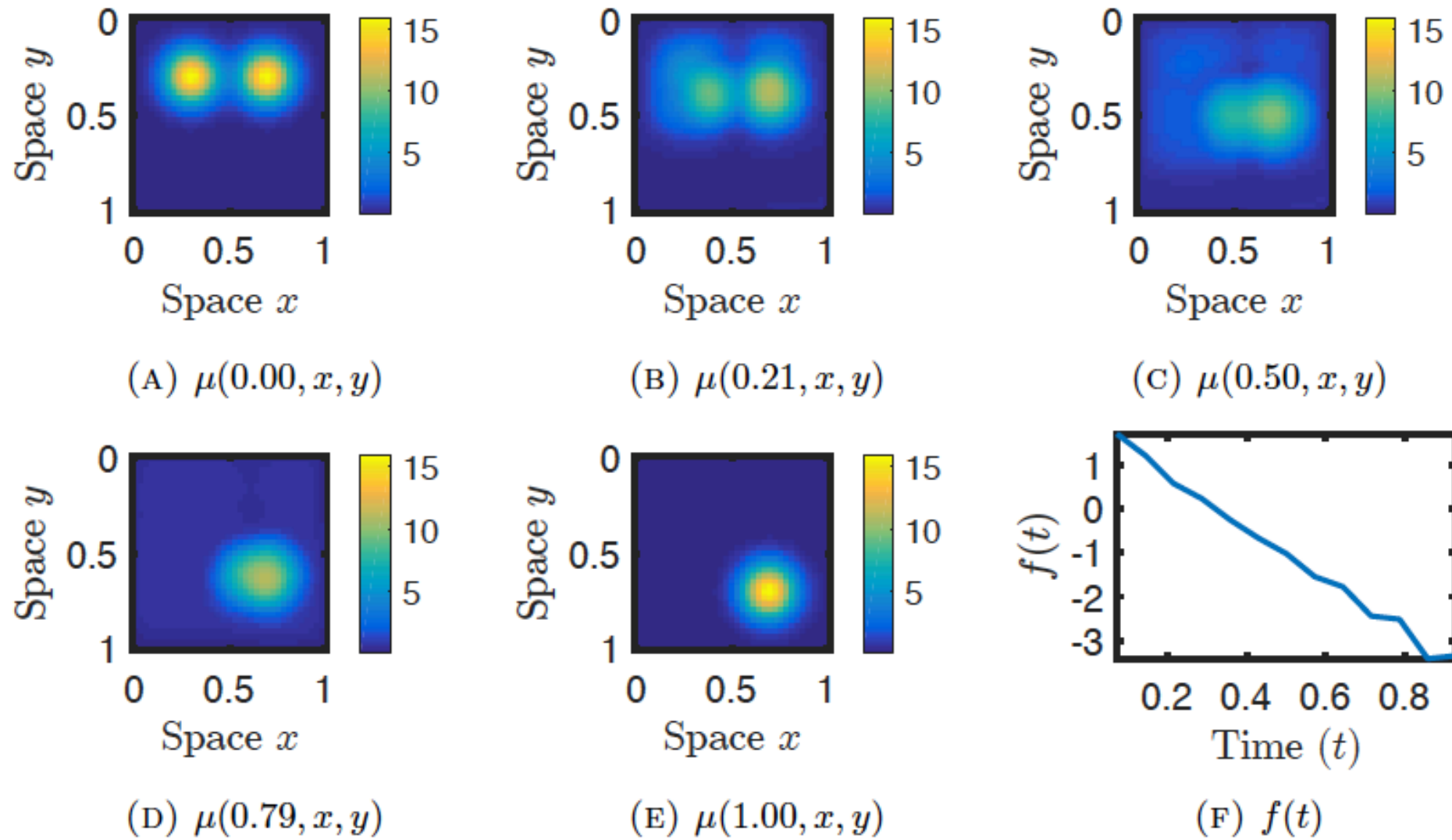


FIGURE 3. Plots of the $u(t, x, y)$ and $f(t)$ for $UW_2(\rho_0, \rho_1)$. (A) $\mu(0.00, x, y)$, (B) $\mu(0.21, x, y)$, (C) $\mu(0.50, x, y)$, (D) $\mu(0.79, x, y)$, (E) $\mu(1.00, x, y)$, (F) $f(t)$.

Example II

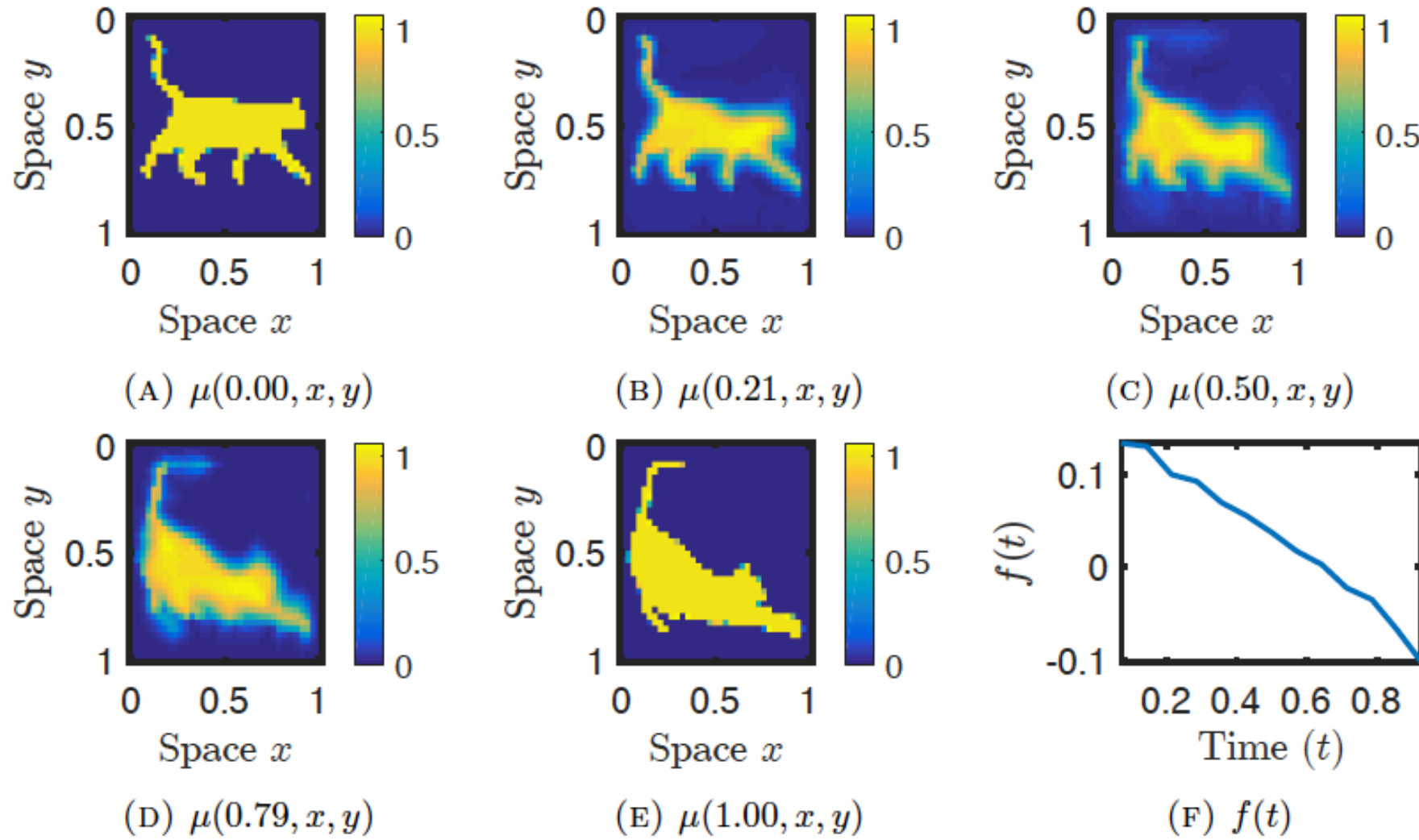
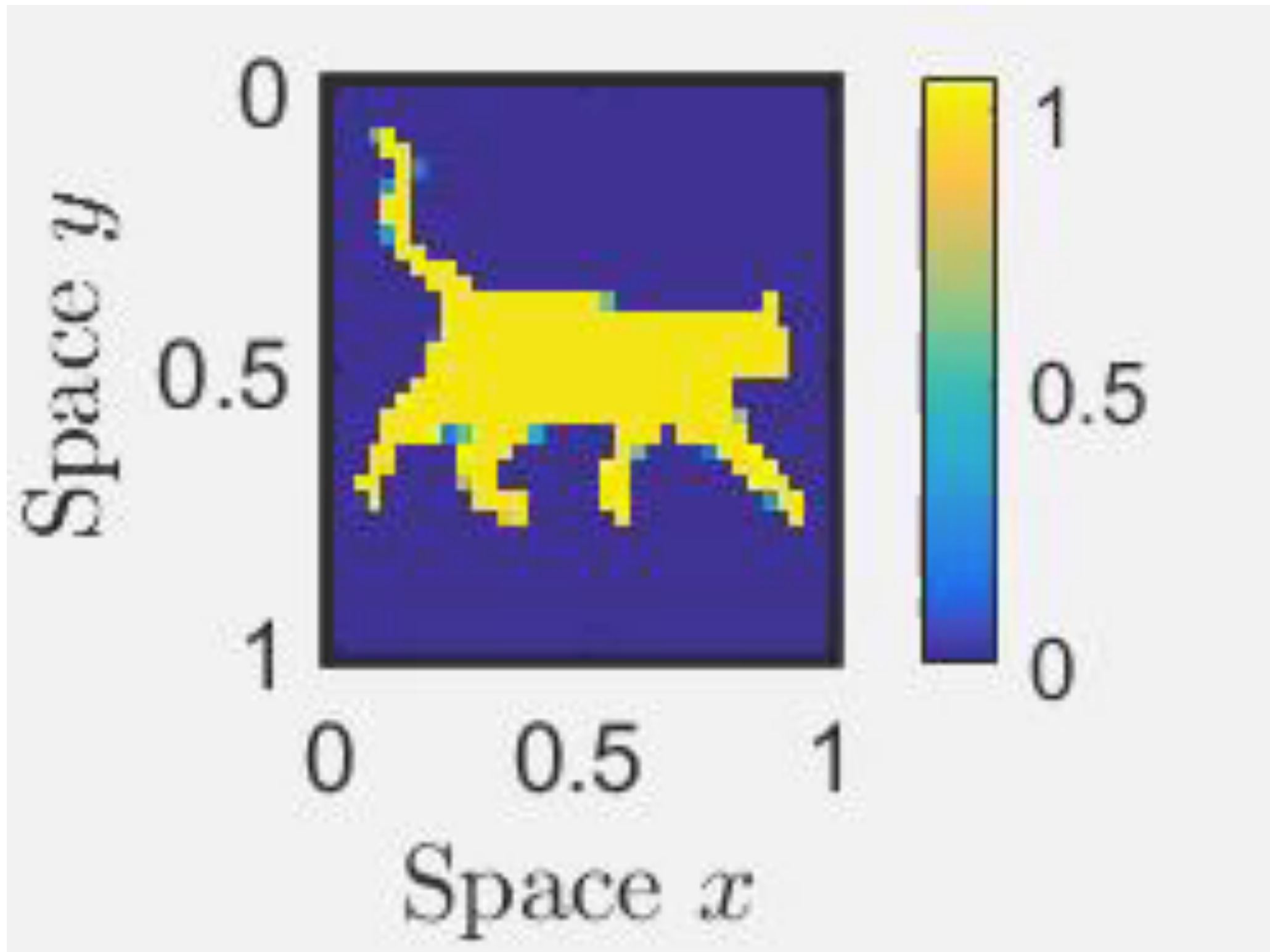


FIGURE 4. Plots of the $u(t, x, y)$ and $f(t)$ for $UW_2(\rho_0, \rho_1)$. (A) $\mu(0.00, x, y)$, (B) $\mu(0.21, x, y)$, (C) $\mu(0.50, x, y)$, (D) $\mu(0.79, x, y)$, (E) $\mu(1.00, x, y)$, (F) $f(t)$.

Example








Discussions

The unnormalized OT opens many interesting fields:

- ▶ Finding closed-form solutions of unnormalized OT;
- ▶ Modeling inverse problem via unnormalized OT;
- ▶ Geometric properties of unnormalized OT;
- ▶ Gradient flows via unnormalized OT;
- ▶ Mean field games and control problems in unnormalized density space.

Main references

-  W. Gangbo, W. Li, S. Osher and M. Puthawala.
Unnormalized Optimal Transport, 2019.
-  M. A. Puthawala, C. D. Hauck, and S. J. Osher.
Diagnosing Forward Operator Error Using Optimal Transport. 2018.
-  Y. Chow, W. Li, S. Osher and W. Yin.
Algorithm for Hamilton-Jacobi equations in density space via a
generalized Hopf formula, 2018.
-  W. Li, P. Yin, and Stanley Osher.
Computations of optimal transport distance with Fisher information
regularization, 2018.
-  W. Li, E. Ryu, S. Osher, W. Yin and W. Gangbo.
A parallel method for Earth mover's distance, 2017.